

MEAN TURBULENT FLOW IN THE WAKE OF A PERFORATED PLATE EQUIPPED WITH NON-THERMAL PLASMA

Nicolas Benard

Institut PPRIME
CNRS - University of Poitiers - ISAE-ENSMA
Bld Marie & Pierre Curie, 86962 Futuroscope France
nicolas.benard@univ-poitiers.fr

Romain Bellanger

Institut PPRIME
CNRS - University of Poitiers - ISAE-ENSMA
Bld Marie & Pierre Curie, 86962 Futuroscope France
romain.bellanger@univ-poitiers.fr

Pierre Audier

Institut PPRIME
CNRS - University of Poitiers - ISAE-ENSMA
Bld Marie & Pierre Curie, 86962 Futuroscope France
pierre.audier@univ-poitiers.fr

Eric Moreau

Institut PPRIME
CNRS - University of Poitiers - ISAE-ENSMA
Bld Marie & Pierre Curie, 86962 Futuroscope France
eric.moreau@univ-poitiers.fr

ABSTRACT

The present experimental contribution interests in the flow field developing downstream of a plate perforated by 121 holes with 1.8-mm inner diameter. The original aspects of this research is that the holes are all surrounded by plasma discharges that can actively impose periodic perturbations to the flow developing in the wake of the plate. In particular, it is shown by flow visualizations and particle image velocimetry that the plasma discharges can significantly affect the turbulent kinetic energy. It is observed that the multi-jet flow quickly form a single jet whose the turbulent production can be significantly increase by operating the plasma discharge in a mode imposing perturbations at a Strouhal number equal to 0.3. This type of forcing promotes an earlier production of turbulence but it also imposes the formation of coherent flow structures with a shedding frequency matching with the one imposed by the actuator.

INTRODUCTION

The mixing of scalar flow component is important for a large number of practical and fundamental situations. Mixing by passively forced turbulence underlies a variety of engineering phenomena, including combustion, injection cooling, industrial mixing and pollution transport. Turbulent sheared flows are well-known for promoting mixing between different streams by a natural amplification of instability waves. Passive systems composed of multiple interfaces in shearing situations can enhance the mixing of turbulent flow. Combustion applications or engineering processes needing a homogeneous mixing of chemical species can find relevant solutions in systems promoting earlier, and controlled turbulent flow characteristics. For instance, the confinement of a fuel jet by lateral shearing regions using lateral oxygen jets results in flame stabilization leading to a significant reduction of pollutant emissions such as NO_x (Boushaki *et al.*, 2008). The use of multiple jets is now quite common in burners because they are effective designs to improve combustion intensity and shorten the length of the flame (Liang *et al.*, 2013). The characterization of these burners is most of the

time limited to a demonstration of the net gain in term of combustion efficiency without particular emphasize on the fluid interfaces caused by the mutual complex interactions between the jets. Recently, the near-field behavior of 6×6 interacting jets has been investigated by mean of PIV and LDA measurements (Ghahremanian *et al.*, 2014). The merging of the jets into a single jet after a certain distance has been qualitatively demonstrated. Indeed, the mutual entrainment between the jets and a low pressure region at the center of the jet array are both responsible for a deflection of the peripheral jets towards the center of the jet array.

The present paper proposes to experimentally detail the mean turbulent flow measured downstream of a ‘multi-jet like’ geometry. One original aspect of the proposed research is the implementation of non-thermal plasma discharges in the multi-jet design. Indeed, the use of plasma actuator, a device particularly useful for imposing periodic flow perturbations at specific frequencies (Benard and Moreau, 2014), opens a large research field related to the active manipulation of the turbulent flow scales in flow geometry with multiple shearing interfaces. This paper presents results from a preliminary flow visualization measurement campaign. Some more recent measurements by high-speed PIV are also presented. They show how plasma actuation can help in modifying the mean turbulent flow and the dynamic of the larger flow structures.

EXPERIMENTAL SETUP

The system is made of a ceramic plate (thickness of 1.27 mm) perforated by 121 holes having an inner diameter of 1.8 mm. The holes are arranged in a way that a circular pattern is defined for this model (Figure 1). The distance between the centers of two successive holes is 3.05 mm (solidity ratio equal to 0.78). A dielectric barrier discharge plasma actuator is included around each hole of the plates. The top of the plasma actuator is made of a conductive layer (nickel with thickness of 10 μm) connected to a high voltage power supply. The grounded electrode is embedded within the ceramic dielectric material at a distance of 630 μm from the air-exposed electrode. The distance between the

edge of an active electrode and the edge of the corresponding

The present contribution focuses on particle image

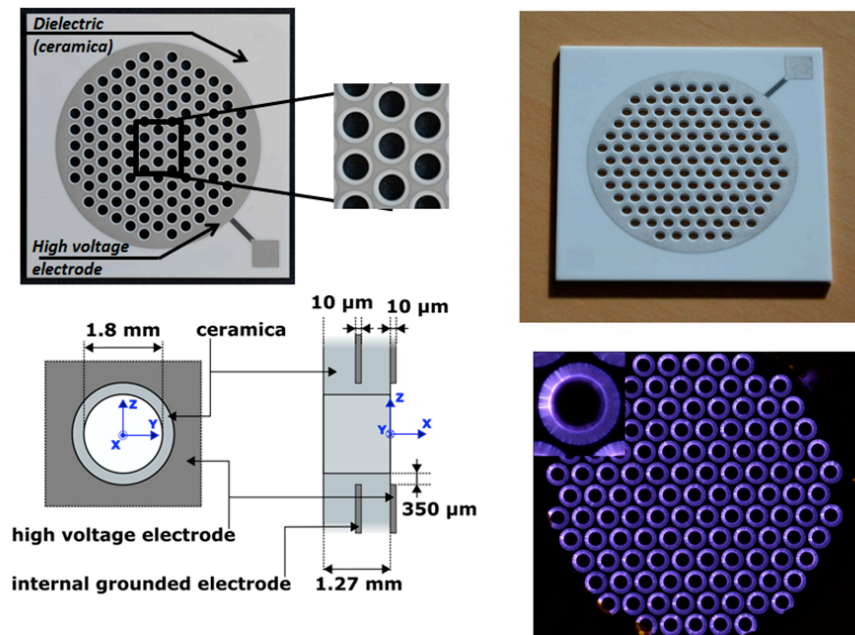


Figure 1. Photographs and sketches (front and slice views) of the perforated plate with non-thermal plasma actuator.

hole designed for the gas passage is $350\ \mu\text{m}$. The plasma discharge is produced by imposing an AC sinusoidal waveform to the top electrode. This waveform results from a 3000 V/V amplification (Trek 30/40). Here, the maximal voltage amplitude is limited to 7.5 kV for an AC frequency of 4000 Hz. At a sufficient onset voltage, the plasma discharge array is fully powered, the electric field producing a visible discharge around each hole (Figure 1). The flow produced by the actuator alone (i.e. in absence of flow passing through the holes) is not documented in this paper but details can be found in Benard et al. (2016). High-resolution PIV has shown that, in the condition described previously, the actuator produce a wall jet in each of the circular holes. This jet is directed toward the negative x direction (i.e., against the main jet direction here) and it has a maximal mean velocity of 2.2 m/s in its center when operated with a voltage amplitude of 7.5 kV and a driving frequency of 2000 Hz. Here the actuator is not used in its continuous mode of forcing. In place, the sinusoidal waveform is bursted by using a gate function allowing us for turning on and off the actuation at low frequency (duty-cycle of 50%). The low time response of the actuator results in a similar mean flow production regardless of the frequency used for the burst modulation. This modulation is necessary to impose low frequency perturbations with sufficient fluctuating amplitudes to affect the flow passing through the holes of the ceramic plate.

The honeycomb plasma discharge has been implemented at the exhaust of a circular open-air type wind-tunnel with a $0.132\ \text{m}^2$ cross-section. This facility has a 1.45 m long chamber, series of mesh grids and a jet exit of 50 mm inner diameter obtained by means of a contraction outlet which improves the flow uniformity (contraction ratio of 1:17). The local velocity (U_0) at the center of one hole of the plasma actuator array is fixed at $20\ \text{m}\cdot\text{s}^{-1}$.

velocimetry measurements of an air flow after its passage through the holes of the perforated plate. A short-pulsed Nd:YLF laser (Terra PIV 527-100-M) has been used. It generates a visible green light ($\lambda = 527\ \text{nm}$) and delivers 30 mJ per oscillator when operated at 1 kHz. A fast camera (Photron APX) is synchronized with the laser for operating the optical diagnostic at 1272 Hz. The laser sheet is placed perpendicularly to the central axis of the honeycomb, this to visualize the flow along its convection in the streamwise direction. For each tests, a flow sequence of 5000 images has been recorded.

RESULTS

Qualitative description of the natural flow

Streamwise and cross-stream views of the flow in absence of plasma discharge are reported in Figure 2. The scale factor of the images in the streamwise plane does not allow us for inspecting in detail the micro-jets issuing from the 1.8 mm holes. In place, the field of view has been chosen for a description of the global jet formed by the interactions between the micro-jets. The visual trace of the micro-jets is only visible in the cross-sectional view. The trace of these jets is more or less well-defined depending on their location. In the central part, they interact together leading to deformed sections (compared to a strictly round jet) due to mutual shearing between the micro-jets streams, but in the outer region of the global jet they are also submitted to a strong shearing and mixing with the outer flow at 'rest', this resulting in a faster dissipation. The structuration of the outer boundary region with mushroom-like vortices resembles the streamwise vortex pairs many times reported in literature for a single round laminar jet (Kozlov et al., 2013) while the structure in the central region of

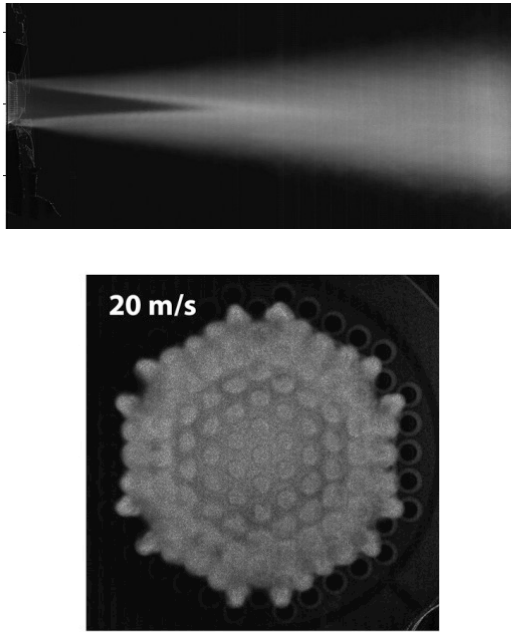


Figure 2. Streamwise ($z/D=0$) and cross-sectional ($x/D=0.5$) flow visualizations of the global jet for flow velocity of $20 \text{ m}\cdot\text{s}^{-1}$.

the jet reminds the structures in coaxial jets where helicoid modes develop (Ivanic et al., 2003). Zoomed views (not shown here, but see in Benard et al., 2015) have shown that the peripheral jets are rapidly deflected toward the axis of the wake flow due to the mutual interactions of the jets as in Ghahremanian et al. (2014). This can also be inferred from the streamwise images where the micro-jets are not aligned with their originating hole due to the peripheral deflection. Finally, the micro-jets evolve into a single jet flow whose potential core can be estimated and surrounding vortex core extracted.

Here, the axial velocity of the global jet reaches $15 \text{ m}\cdot\text{s}^{-1}$ and the potential core is of about 178 mm. The global jet has a width, D , equal to 28.8 mm. This diameter can be used to rescale the measured quantities. It is observed that the potential core length corresponds to $6.2D$, a value in agreement with the expected length for a turbulent jet flow ($Re_D=28500$).

Influence of the plasma discharge on the mean global jet flow

In Benard et al. (2016), it has been shown that the potential core length can be significantly reduced by turning on the plasma discharge. A strong dependency on the frequency of modulation has been observed. Results extracted from flow visualizations are summarized in Figure 3. It is shown that the potential core of the global jet can be reduced down to $3.7D$. The reduction in potential core length is obviously accompanied by a larger spreading rate of the jet as shown in the flow visualization proposed in Figure 3. The larger reduction is reported for an excitation at $St_D=0.32$, a forcing condition close to the well-known best periodic forcing that excites the instability of the jet

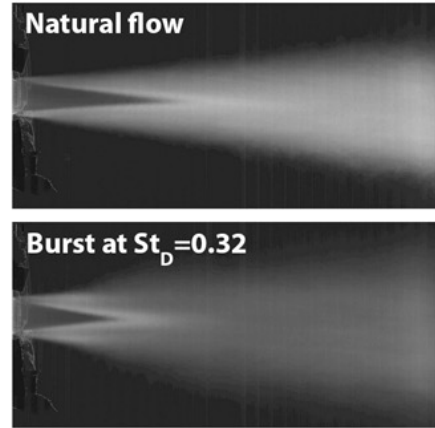
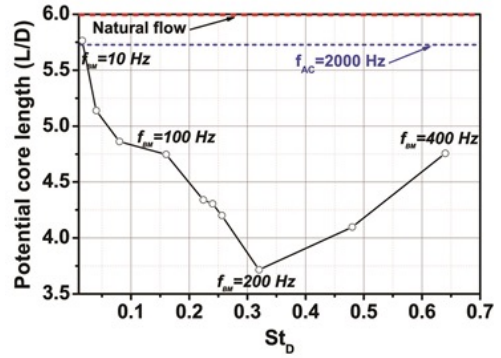


Figure 3. Reduction in the potential core length obtained for jet flows at $U_0=20 \text{ m}\cdot\text{s}^{-1}$ and comparison of the mean flow for natural flow and the most effective control at $St_D \approx 0.3$.

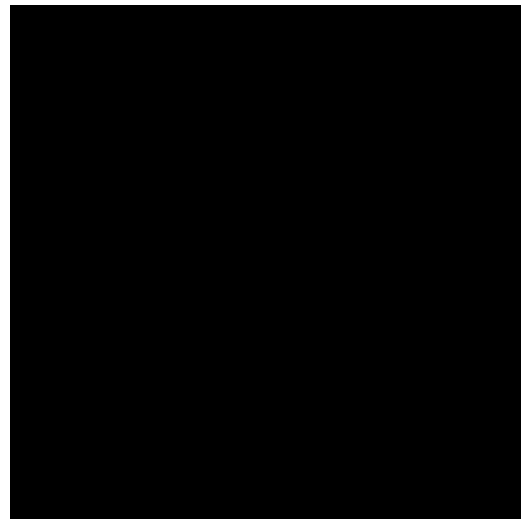


Figure 4. Mean flow in $\text{m}\cdot\text{s}^{-1}$ for natural flow and forcing frequencies at $St_D=0.3$.

column mode or preferred mode of a turbulent jet (Zaman and

actuator. In order to identify the capability of the actuator for



Figure 5. Spatial distribution of the turbulent kinetic energy (in $m^2.s^{-2}$) for natural flow and different forcing frequencies.

Hussain, 1980).

Measurements by high-speed PIV have been conducted giving precise quantifications of the flow changes imposed by the plasma actuator. The mean flow for the baseline conditions and an actuation at the 'optimal' frequency 0.3 is illustrated in Figure 4. This quantitative measurement gives confidence in the jet core length reduction reported from the flow visualizations and it confirms the increase in spreading rate caused by the plasma

increasing the turbulent quantities, the spatial distributions of the turbulent kinetic energy have been computed and compared for different flow conditions (Figure 5). The turbulent kinetic energy is high in the outer region of the jet where primary and secondary flow structures develop and interact with the surrounding air. In case of actuation, the plasma discharge systematically amplifies and enlarges the region of high turbulence. A strong effect is reported for $St_D=0.3$ with a spectacular increase in the turbulence

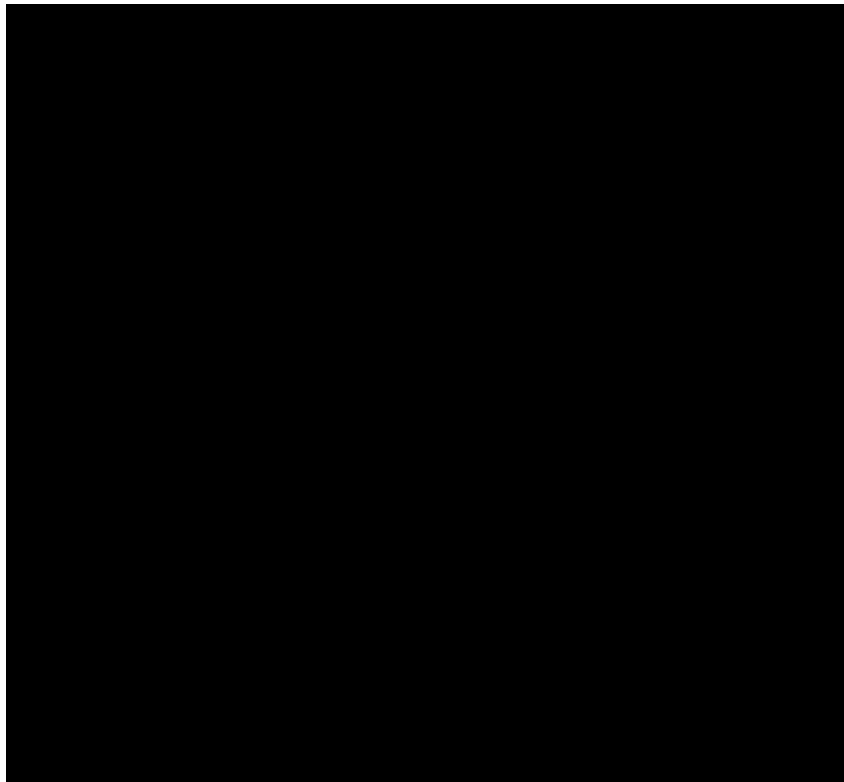


Figure 6. Reynold stress components for natural and flow forced at $St_D=0.3$.

level.

Three components of the Reynolds stress tensor are presented in Figure 6. Each of the components is modified by the actuation but in a different manner. The RS_{xx} component is reduced in amplitude but its distribution shows an earlier deflection of the peripheral region. The transverse RS_{yy} component is strongly reinforced, but the noticeable point is the high RS amplitude very close to the perforated plate. The turbulent transfers in the oblique direction reflect the deflection of the micro-jets and the high turbulent activity downstream of the potential core.

Influence of the plasma discharge on the jet flow dynamic and flow structures

The use of a high-speed PIV system allows us for inspecting the time-resolved flow. A short sequence of images with flow seeded by reflecting particles is shown in Figure 7. It clearly highlights the large change in the flow topology when plasma actuator is turned on. The reduction in the potential core length is evidenced in this figure, as well as the formation of large scale flow structures growing from the origin to the end of the potential core.

The changes in the flow organization are also estimated by a phase-averaging procedure applied to the high-speed PIV velocity fields. The acquisition rate of the PIV system has been adapted regarding the physical burst frequency. Here, for forcing at $St_D=0.3$, the physical frequency is 212 Hz. The PIV system is synchronized at 1272 Hz, thus a forcing period can be easily discretized into 6 phases. Each phase average is computed using 600 velocity fields. This procedure is a form of triple flow decomposition as originally proposed by Reynolds and Hussain

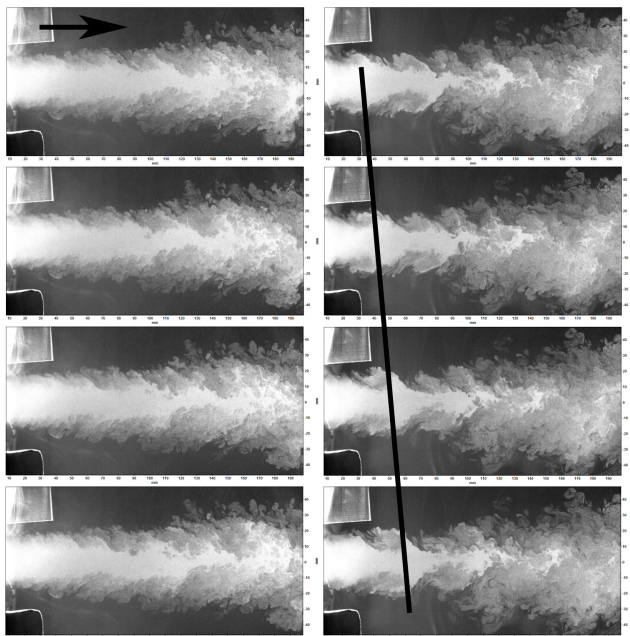


Figure 7. Smoke flow visualizations for natural (left) and controlled flow at $St_D=0.3$ (right). Successives images are separated by a time delay of 786 μ s.

(1972):

$$u(x,t) = \bar{u}(x) + \overline{u'(x, \varphi(t))} + u'(x,t) \quad (1)$$

where u is one of the two measured velocity components, \bar{u} is its mean value, $\overline{u'}$ is the phase dependent part (with φ , the phase angle) while u' corresponds to the stochastic turbulent part of the instantaneous flow field u . The phase-averaging procedure can only be applied to the controlled flow cases. The influence of the forcing conditions on the coherent part of the turbulent flow can be highlighted, but the procedure can also provide a statistical description of the flow dynamics assuming that the manipulated flow is periodic. The mean flow fields at each phase are post-processed in order to extract the larger flow structure in the measurement plane. The λ_2 -criterion, as it was originally defined by Jeong and Hussain (1995), has been chosen among other techniques for an effective extraction of the region of low pressure, a region that can be suspected to be a vortex center. The results for a forcing period (at $St_D=0.3$) are shown in Figure 8. They confirm the highly periodic flow organization when the actuator is operated. The phase-averaging procedure leads to the identification of well-defined flow structures whose size increases while they are convected. The growing mechanism of these flow structures is dominated by fluid entrainment because no trace of vortex pairing emerges from the phase-averaged flow fields. The flow structures are continuously reinforced when they are convected, this up to $x/h \approx 3$ position (i.e., the end of the potential core). Beyond this point, the large scale flow structures are quickly dissipated this contributing to a sudden spreading rate increase of the jet.

CONCLUSION

The mean flow developing downstream of a perforated plate equipped with plasma discharge has been characterized by smoke flow visualization and PIV. It was shown that the micro-jets collapses to form a global jet that is highly sensitive to the frequency imposed by the actuator. By imparting periodic fluctuations at $St_D=0.3$, the jet core length can be minimized and the mixing further increase.

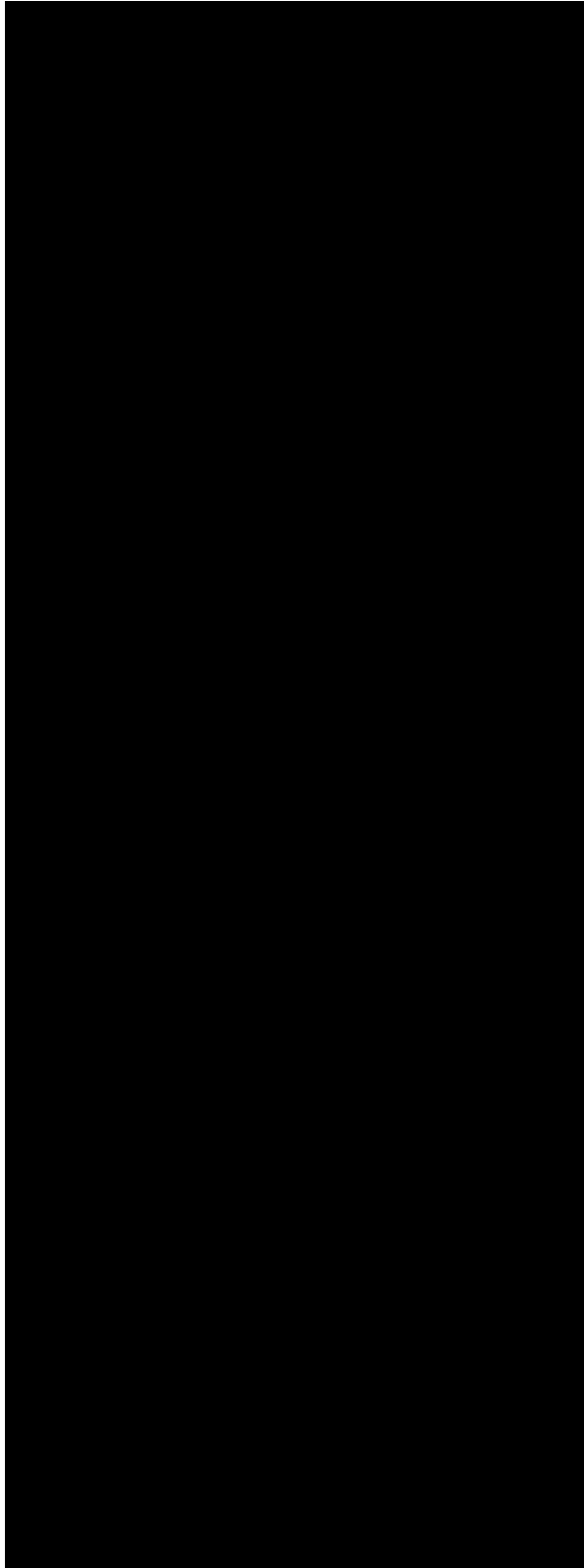
This study is the first step of a more global investigation on turbulent flow control by coupling a passive grid and an active actuator without mechanical part. Such a coupling opens exciting new researches in fluid mechanics, turbulence and combustion.

ACKNOWLEDGEMENTS

The equipment used in this work was funded by the French Government program "Investissements d'Avenir" (LABEX INTERACTIFS, reference ANR-11-LABX-0017-01). This work is conducted under DGA supervision.

REFERENCES

Benard N., Mizuno A., and Moreau E., 2015, "Manipulation of a grid-generated mixing with an active honeycomb dielectric barrier plasma discharge", *Applied Physics Letter*, Vol. 107



Benard, N., Mizuno, A., and Moreau, E., 2016, "Active Multiple Jets System Using Surface Plasma Actuator", *8th AIAA Flow Control Conference*, AIAA paper 2016-3775

Benard N., and Moreau, E., 2014, "Electrical and mechanical characteristics of surface AC dielectric barrier discharge plasma actuators applied to airflow control", *Experiments in Fluids*, Vol. 55, 1846

Boushaki, T., Mergheni, M.A., Sautet, J.C., and Labegorre B., 2008, "Effects of inclined jets on turbulent oxy-flame characteristics in a triple jet burner", *Exp. Thermal Fluid Sci.*, Vol. 32, pp: 1363-1370

Ghahremanian, S., Svensson, K., Tummers, M.J., and Moshfegh, B., 2014, "Near-field development of a row of round jets at low Reynolds numbers", *Experiments in Fluids*, Vol. 55, pp: 1789

Kozlov, V.V., Grek, G.R., Dovgal, A.V., and Litvinenko, Y.A., 2013 "Stability of subsonic jet flows", *J. of Flow control, Measurement & Visualization*, Vol. 1, pp: 94-101.

Ivanic T., Foucault E., and Pecheux J., 2003, "Dynamics of swirling jet flows", *Experiments Fluids*, Vol. 35, pp: 317-324.

Jeong J., and Hussain F., 1995, "On the Identification of a Vortex", *Journal of Fluid Mechanics*, Vol. 285, pp: 69-94.

Liang, Q.F., Guo, Q.H., Yu, G.S., and Wang, F.C., 2013, "An experimental investigation on characteristics of individual flame and multi-jet flame", *Energy Sources*, Vol. 35, pp: 1476-1485

Reynolds W.C., and Hussain A.K.M.F., 1972, "The mechanics of an organized wave in turbulent shear flow. Part 3. Theoretical models and comparisons with experiments", *Journal of Fluid Mechanics*, Vol. 54, pp:263-288.

Zaman, K.B.M.Q., and Hussain, A.K.M.F. 1980, "Vortex pairing in a circular jet under controlled excitation. Part 1: General jet response", *Journal of Fluid Mechanics*, Vol. 101, pp. 449-491

Figure 8. Phase-averaged description of the vortical flow structures identified by a negative λ_2 criterion for plasma actuator operated at $St_D=0.3$. The images are separated by a phase angle of $2\pi/6$ ($\Delta t=4.7$ ms).